Emission dynamics of an expanding ultrafast-laser produced Zn plasma under different ambient pressures

N. Smijesh and Reji Philip[a)]
Raman Research Institute, C.V. Raman Avenue, Sadashivanagar, Bangalore 560080, India

(Received 15 June 2013; accepted 22 August 2013; published online 6 September 2013)

We report time and space resolved spectral measurements of neutral Zn emission from an ultrafast laser produced plasma, generated by the irradiation of a Zn target with laser pulses of 100 femtoseconds duration, carried out in a broad ambient pressure range of 0.05 to 100 Torr. The measurement is done for three different axial positions in the expanding plume. The spectra are rich in neutral Zn (Zn I) emissions at 334.5 nm, 468 nm, 472 nm, 481 nm, and 636 nm, respectively, depicting the characteristic triplet structure of Zn. Fast as well as slow peaks are observed in the time of flight data of 481 nm emission, which arise from recombination and atomic contributions, respectively, occurring at different time scales. Average speeds of the fast atomic species do not change appreciably with ambient pressure. The plasma parameters (electron temperature and number density) are evaluated from the measured optical emission spectra. The rates of ionization and recombination can be enhanced by a double-pulse excitation configuration in which optical energy is coupled to the ultrafast plasma through a delayed laser pulse. © *2013 AIP Publishing LLC*. [http://dx.doi.org/10.1063/1.4820575]

INTRODUCTION

Interaction of laser pulses with solid targets and the subsequent evaporation of material from the target surface, namely laser ablation, has received substantial attention from the scientific community recently. Intense laser excitation leaves the ablated material in a highly excited plasma state, wherein a rapid formation of fast ions, atoms, and nanoparticles[1–5] take place. In particular, ultrafast laser ablation is a preferred technique to generate an intense plasma that contains high energy radiation such as high harmonics[6,7] and X-rays.[8] Notwithstanding the target properties and surrounding pressures,[9] laser ablation and plasma production are dependent on various laser parameters such as pulse energy, pulse duration,[10] wavelength,[11] and laser fluence.[12] Unlike nanosecond (ns) laser pulses, sub-picosecond ultrafast laser pulses do not interact with the plasmas produced by them because electron-ion interaction and heat conduction happen at timescales typically ranging from a few picoseconds onwards. Therefore, the entire energy content of the pulse is deposited on the target resulting in efficient material ablation[10] and plasma formation. This leads to a different emission dynamics in femtosecond (fs) laser produced plasma (LPP) compared to nanosecond (ns) LPP. Theories of ns plasma formation and expansion reveal that a blast wave model[13] is the best available description for moderate pressures while the shock wave model is appropriate for lower pressures.[14] At extremely low pressures, a molecular dynamics simulation can fit the experimental data. Unlike short-pulse (ns) excitation, ultrafast excitation minimizes the possibility of ejected particles interacting with the laser field, and thereby prevents further ionization. This effect reduces the complexity of fs ablation compared to nanosecond laser ablation.[15] Thus, the theoretical model used for describing ns LPP is not strictly applicable to the fs ablation mechanism. The two available descriptions for ablation by ultrashort pulses are the plasma-annealing model and the two-temperature model.[15,16]

Conventional techniques employed for the observation and analysis of fs plasma include ion probe studies and time-resolved and time-gated emission spectroscopy. It has been shown experimentally that ultrafast laser plasma plumes consist of fast ions, neutral atoms, and nanoparticles, and that plume expansion depends on ambient conditions and initial parameters.[17] Growth from nanoparticles to nanoclusters in the later stages of plume expansion can be characterized by diffusion limited aggregation.[15,18] The plume acts as a black body radiator at the later stages of expansion due to the formation of nanoparticles. Compared to short-pulse excitation, the ultrafast LPP plume has a relatively complex structure, even though the processes leading to plume formation are simpler.

In the present work, we have carried out spectroscopic and time evolution studies of Zn plasma produced by the irradiation of a high purity Zn target by 796 nm, 100 fs laser pulses of fluence ~16 Jcm^{-2}. Plasma parameters such as electron temperature and number density are calculated for various pressures using the relative emission line intensity ratios and the Stark broadening mechanism, respectively. The time evolution of spectral intensity at 481 nm is measured for determining the emission dynamics of neutral Zn species. Spatial information is recorded by scanning the plasma plume along its length, which is repeated for various ambient (nitrogen) pressures. Atomic emission is more prominent in the Zn plasma plume at higher pressures. It is found that ionization and recombination mechanisms can be enhanced by employing a double-pulse excitation configuration.

[a)]E-mail: reji@rri.res.in

EXPERIMENTAL

The excitation source was a regeneratively amplified ultrafast Ti:Sapphire laser (*TSA-10, Spectra Physics)* operating at 796 nm, pumped by a Q-Switched Nd:YAG laser, and seeded by a mode-locked Ti:Sapphire oscillator *(Tsunami, Spectra Physics)*. Maximum laser pulse energy is 10 mJ. The pulse width of the laser is ~100 fs, which is monitored using an autocorrelator (*SSA-F*, *Positive Light*). A high resolution (0.06 nm) spectrometer *(iHR 320, Horiba Jobin Yvon*) fitted with a CCD detector (*Synapse*) and photomultiplier tube (*R943-02*, *Hamamatsu*) was employed for emission spectral recording and time-resolved studies. Laser pulses attenuated to approximately 5 mJ energy are focused on to the surface of the target to produce the plasma (laser fluence ~16 Jcm^{-2} and power density ~ 1.6×10^{14} Wcm^{-2}). The target is a Zn plate of purity better than 99.99% (ACI Alloys Inc.). The laser is set to run at 10 Hz for energy stability, but plasma measurements are taken in the single-shot mode using a fast mechanical shutter placed in the beam path, which opens only when required. An electronic synchronization circuit is used to drive the shutter, so that single pulses (SPs) can be selected from the 10 Hz pulse train at will. In order to avoid pitting of the target surface, after each laser pulse, the sample is moved by about 1 mm using a stepper motor driven X-Y translator, so that the following laser pulse falls on a new point on the target surface. The plasma plume was studied with the help of an imaging system, which can be moved horizontally to observe different axial positions of the plume, in order to get spatial information. The recorded spectral lines are identified by comparison with the standard NIST atomic spectra database.[19] Time evolution data from the photomultiplier tube (PMT) were recorded on a fast oscilloscope *(DPO 7354, Tektronix*).

RESULTS AND ANALYSIS

Optical emission spectra recorded at distances of 2 mm, 4 mm, and 6 mm from the target surface, measured axially along the expansion direction of the plume, are shown in Fig. 1. Though the wavelength spectrum is essentially unchanged, emission intensity gets reduced by two orders of magnitude due to the above 4 mm translation (from 2 mm to 6 mm) along the plume axis. Neutral Zn (Zn I) emissions are found at 334.5 nm, 468 nm, 472 nm, 481 nm, and 636 nm, respectively, depicting the characteristic triplet structure[20] of Zn. Lines from ionized Zn (Zn II) are visible at 491 nm, 492 nm, 589 nm, and 610 nm, but these are less intense compared to Zn I emission.

Emission intensity—especially from the ionized species—is found to vary with ambient pressure. Variation of emission intensity for ionized as well as neutral species, measured 2 mm away from the target surface, is shown in Fig. 2. At low pressures, the plume expands more, reducing the number density and collisions, and therefore, the ionization rate. As the pressure increases, self-focusing of the beam and multi-photon ionization of ambient gas will occur, reducing the energy reaching the target.[21] This results in a reduction in the mass of the ablated material. But on the other hand, the collision rate increases, leading to enhanced

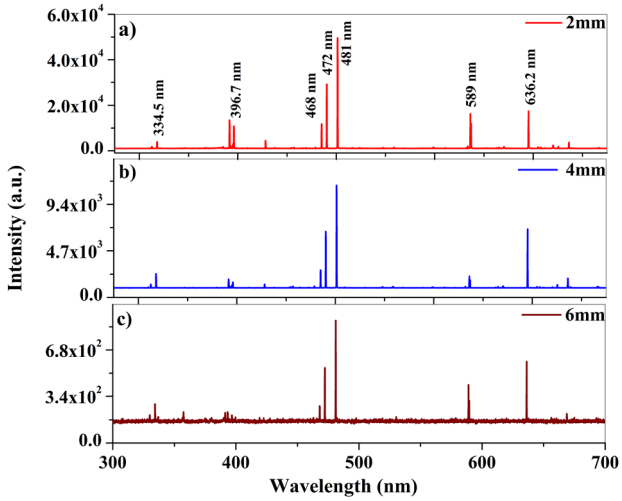

FIG. 1. Emission in the visible region from an ultrafast Zn plasma produced by the irradiation of a Zn target by 100 fs laser pulses at 796 nm. The plume is imaged at distances of 2 mm, 4 mm, and 6 mm, respectively, from the target surface, along the expansion direction. Ambient pressure is 10 Torr.

ionization of the ablated species. As a result of these competing processes, the emission intensity peaks at a certain intermediate pressure. In the present case, emission peaks around an ambient pressure of 10 Torr, because it is the optimum pressure for maximum emission at a distance of 2 mm from the target surface.

Calculation of plasma parameters (electron temperature and number density) was done by conventional methods as follows. Electron temperatures (T_e) were evaluated using the line emission intensity ratios of Zn I emissions at 334.5 nm ($4s4d\ ^3D_3 - 4s4p\ ^3P_2$) and 481.0 nm ($4s5s\ ^3S_1 - 4s4p\ ^3P_2$) by assuming local thermodynamic equilibrium (LTE) using the equation

$$\frac{I_1}{I_2} = \frac{g_1}{g_2}\frac{A_1}{A_2}\frac{\lambda_2}{\lambda_1}\exp\left[\frac{-(E_1 - E_2)}{K_B T_e}\right], \tag{1}$$

where λ_i, A_i, g_i, I_i, and E_i ($i = 1,2$) are the wavelength, transition probability, statistical weight, line intensity, and energy of the excited state, respectively. The spectroscopic constants (A_i and g_i) were taken from a reported work.[20] An evaluation of the electron number density (N_e) was done from Stark broadening of line emission at 481 nm (neglecting ion contribution to line broadening) at each pressure, using the equation[22,23]

$$\Delta\lambda_{1/2} = 2\omega\left(\frac{N_e}{10^{16}}\right), \tag{2}$$

where $\Delta\lambda_{1/2}$ is the full width at half maximum (FWHM) of emission and ω is the electron impact parameter. The theoretical value of ω was obtained from literature.[24] A Lorentzian fit to the emission profile at 481 nm, measured 2 mm away from target surface at an ambient pressure of 10 Torr, is shown in Figure 3. Calculated values of T_e and N_e for various ambient pressures, at different distances in the plume from the target surface, are shown in Table I. The validity of LTE was checked using the McWhirter criterion[25] for each pressure, i.e.,

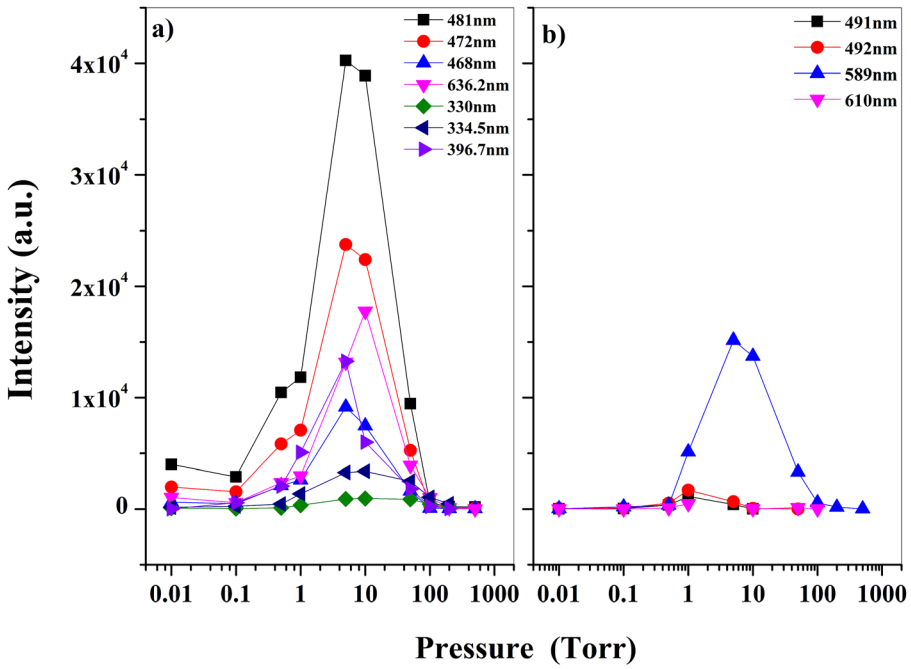

FIG. 2. Variation of emission intensity with ambient pressure (plotted in the log scale) for different plasma spectral lines, measured 2 mm away from the target surface. (a) Zn I species and (b) Zn II species.

$$N_e \geq 1.6 \times 10^{14} T_e^{0.5} (\Delta E)^3 \text{cm}^{-3}, \quad (3)$$

which gives a value of 2.4×10^{15} in the present case.

Obviously, the species velocities play an important role in the emission properties of the plume, which moves rapidly, radiating in the visible, UV, and X-ray spectral regions. We carried out time of flight measurements (TOF) to measure the time evolution of the plasma under different ambient pressures. Measurements were done for distances of 2 mm, 4 mm, and 6 mm from the target surface, for an ambient pressure range of 0.05 to 100 Torr. Results are shown in Figs. 4(a)–4(c), respectively. Since the electric field corresponding to the laser pulse intensity is $\sim 3.5 \times 10^{10}$ Vm^{-1}, which is above the threshold for Coulomb explosion (1.173×10^{10} Vm^{-1}), the target surface vaporises directly upon irradiation by the femtosecond pulse.[26] Thus, material ablation happens almost instantaneously as the excitation pulse hits the Zn target, and the ejected species expand until the pressures within and outside the plume are balanced. When expanded adiabatically, fast species within the femtosecond plasma move with an average speed $\sim$100 kms^{-1} while slow species move at $\sim$1–10 kms^{-1}. The number density falls away from the target surface, leading to diminishing plume size.

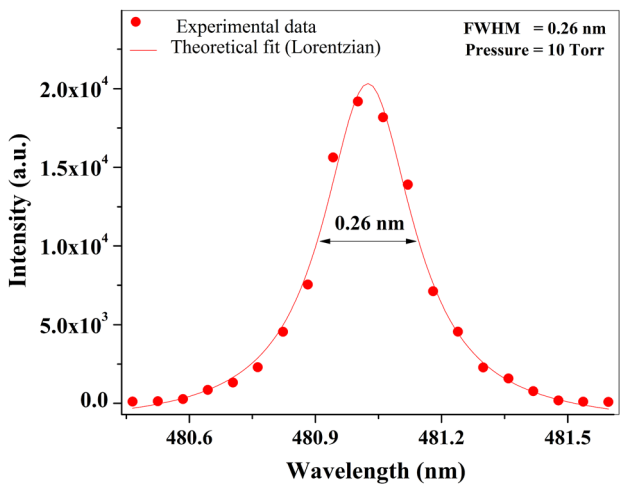

FIG. 3. Lorentzian fit to the Zn I emission profile at 481 nm recorded at 10 Torr, measured at a distance of 2 mm from the target surface. The FWHM is 0.26 nm.

As seen from Fig. 4, all TOF spectra exhibit one sharp peak (PK1) first, the intensity of which increases steadily with pressure at the 2 mm position. PK1 is found to have a consistent time delay, which is rather independent of the ambient pressure. Therefore, it may be suspected that PK1 is a photopeak: however, if the spectrometer setting is changed by 1 nm either to 480 nm or 482 nm, the peak disappears. This confirms that PK1 indeed indicates fast atomic species, which is zooming past as the leading edge of the plasma plume. In fact, this peak arises from the recombination of the fast ions with electrons in the early stages of plasma plume evolution. These ions are ejected normal to the target surface, and measurements show that at 10 Torr pressure, they are accelerating with average velocities of 57 ± 2 kms^{-1}, 109 ± 9 kms^{-1}, and 154 ± 12 kms^{-1}, respectively, at the 2 mm, 4 mm, and 6 mm positions in the plume. This acceleration is caused by the electron cloud which moves faster than the ion cloud in the plasma: the electric field created by the electrons attracts the ions that follow, some of which recombine with the electrons to form neutral atoms. Sources of error in the velocity calculation are the accuracy of positioning of the imaging system ($\pm$10 microns) and accuracy of readout from the oscilloscope ($\pm$1% of full scale reading). Velocities measured for different ambient pressures are given in Fig. 5. PK1 is followed by a stronger and broader peak PK2, which, unlike PK1, becomes weaker at higher pressures and disappears altogether at the highest pressures studied. Similarly, the average velocity of the relatively

TABLE I. Electron temperature (T_e) and number density (N_e) of the plasma, calculated for different ambient pressures, at increasing distances from the target surface. LTE is found to be valid in all cases.

	2 mm		4 mm		6 mm	
Pressure (Torr)	T_e (K)	N_e (cm^{-3}) ($\times 10^{15}$)	T_e (K)	N_e (cm^{-3}) ($\times 10^{15}$)	T_e (K)	N_e (cm^{-3}) ($\times 10^{15}$)
0.05	6826 ± 193	3.32 ± 0.16	5767 ± 259	3.29 ± 0.22	5472 ± 31	3.16 ± 0.14
0.5	6406 ± 646	3.26 ± 0.74	4356 ± 303	3.17 ± 0.10	4005 ± 70	3.16 ± 0.15
0.1	4987 ± 82	3.56 ± 0.29	4725 ± 10	3.29 ± 0.22	4705 ± 147	3.18 ± 0.16
1	5248 ± 160	3.82 ± 0.44	4900 ± 157	3.24 ± 0.12	4572 ± 14	3.16 ± 0.10
10	8754 ± 695	3.88 ± 0.70	8844 ± 34	3.32 ± 0.42	8727 ± 283	2.73 ± 0.17

long-lived PK2 drops from 10 kms^{-1} to 2 kms^{-1} as the pressure is increased from 0.05 Torr to 10 Torr. Adiabatic expansion of the plume consequent to intense ultrafast excitation results in a quick reduction of emission intensity away from the target surface. As seen from Fig. 2, maximum emission is found at the optimum pressure of 10 Torr for the 2 mm position.

The processes involved in fs plasma plume formation are simpler compared to those of ns plasma plume formation,[3] but the dynamics of emission is rather complex as revealed by the TOF spectra. It is clear from Fig. 4 that the pressure range of 0.05 Torr to 10 Torr is the regime in which the plasma plume experiences turbulence during expansion. This is because of the competing processes prevalent at these pressures. On the one hand, large number densities ensure that collisions and thereby ionization are maximized, while on the other hand, recombination of faster ions with electrons enhances optical emission from neutrals at 481 nm. Line emission lasts up to ~0.9 μs, 5 μs, and 3 μs, at the 2 mm, 4 mm, and 6 mm positions, respectively. The ablation threshold, which is defined as the minimum power density required for vaporizing the material, is given by[27]

$$I_{min} = \frac{\rho L_\nu k^{\frac{1}{2}}}{\Delta t^{\frac{1}{2}}}, \tag{4}$$

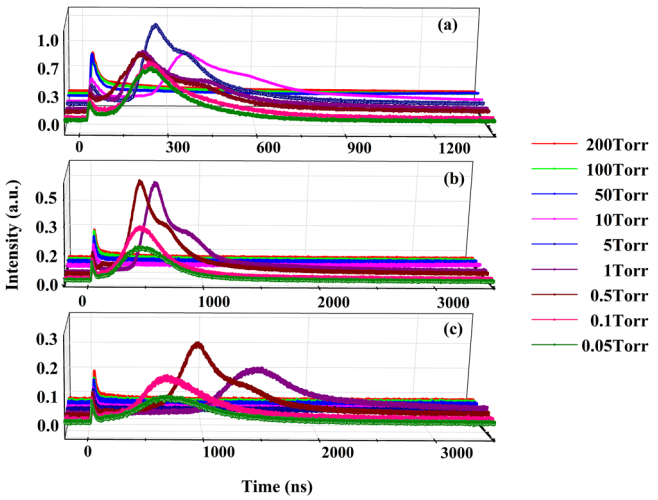

FIG. 4. Time Resolved emission of the 481 nm ($4s5s\ ^3S_1 \rightarrow 4s4p\ ^3P_2$) line of Zn I at different ambient pressures, measured in the plasma plume at distances of (a) 2 mm, (b) 4 mm, and (c) 6 mm, respectively, from the target surface.

where ρ is the density of the material, L_v is the latent heat of vaporization, k is the thermal diffusivity, and Δt is the laser pulse width. I_{min} can be calculated as 2.77×10^{10} W/cm^2 in the present case, and the corresponding laser fluence is 2.77×10^{-3} J/cm^2. With a laser fluence of ~16 Jcm^{-2} which is way above the ablation threshold, an efficient ablation of the target material happens rapidly, and a shock wave propagates back and forth through the ambient gas,[15] introducing a peak shift at certain pressures in the TOF. This also results in a small third peak, PK3, which appears as a wing to PK2 at lower pressures as seen in Fig. 4. PK2 and PK3 disappear at higher pressures indicating that plume expansion is hindered due to the plasma confinement effect.

We also carried out a double pulse (DP) experiment in which a 2 mJ pulse was fired into a plasma plume, which was generated 4 ns earlier by a 5 mJ laser pulse. To generate these pulses, the laser was run at full energy (10 mJ) and the beam was initially divided into two using a 1:1 beam splitter. One of the beams was then sent through a delay stage, and attenuated to 2 mJ using a half-wave plate-polarizer cube combination. The TOF data for single pulse (SP) and DP excitations for 5 Torr background, at 2 mm and 4 mm distances from the target surface respectively, are shown in Fig. 6. The TOF dynamics reveals that the relative time of arrival of the fast component (PK1) is unaffected by double pulse excitation: however, the slow species (PK2) is accelerated upon irradiation with the second pulse. DP excitation facilitates coupling of laser energy to the plasma plume in the ultrafast

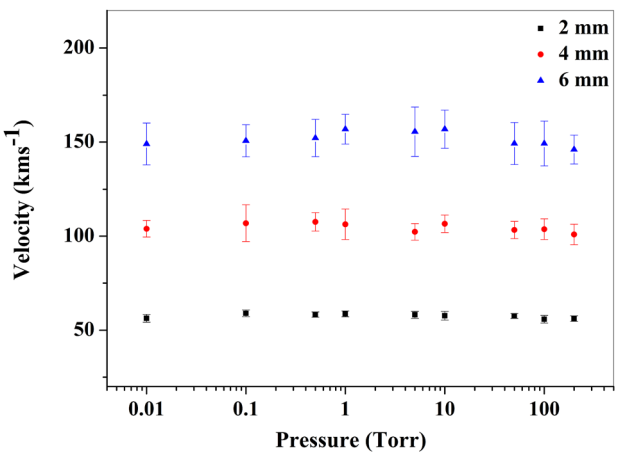

FIG. 5. Velocity of PK1 at different distances from the target surface, measured for the ambient pressure range of 0.01 to 200 Torr. Error bars were obtained from multiple measurements.

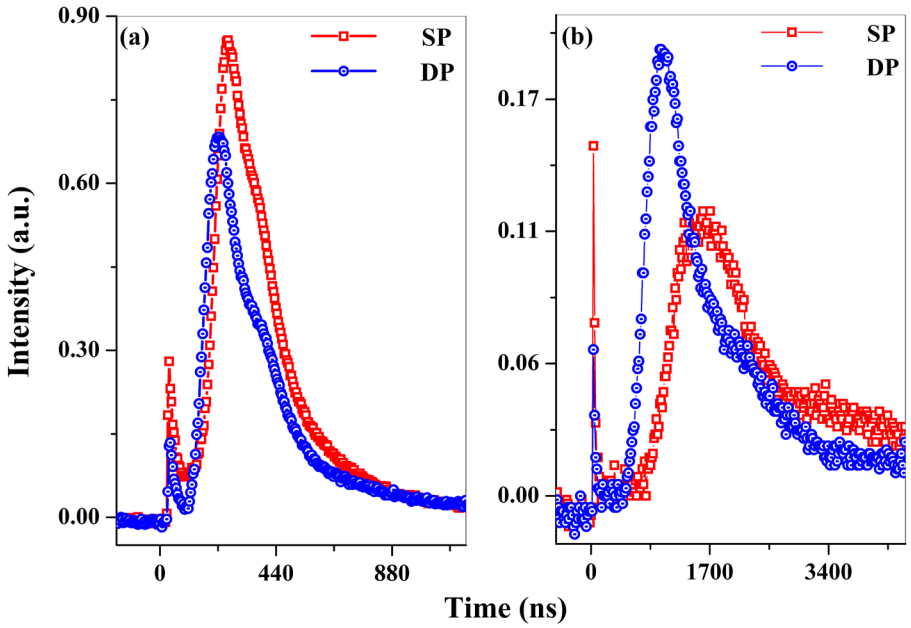

FIG. 6. TOF spectra of 481 nm emission from Zn I at an ambient pressure of 5 Torr, measured using SP and DP excitations, at distances (a) 2 mm and (b) 4 mm from the target surface.

excitation domain: energy is coupled to the fast atomic species with the present delay time of 4 ns, leading to a reduction in its emission intensity. In the DP configuration, the TOF signal intensity of PK2 is found to be nearly doubled at the 4 mm position compared to SP excitation, while it is halved for PK1 at the 2 mm and 4 mm positions. The DP plume decays faster than the SP plume as well. Further measurements are in progress to investigate the finer aspects of ultrafast DP excitation of a laser produced Zn plasma.

CONCLUSION

In summary, we have carried out laser induced breakdown spectroscopy and time of flight measurements of an ultrafast (100 fs) laser produced Zn plasma, generated by irradiating a Zn target using 5 mJ, 100 fs, 796 nm laser pulses. Time of flight measurements of neutral Zn species have been carried out using the 481 nm line emission from the plasma. The electron temperature and number density of the ultrafast LPP have been calculated for different axial positions of the plume. Measurements have been performed over a broad range of ambient pressures, extending from 0.05 Torr to 100 Torr. The emission intensity decays by two orders of magnitude within a distance of 6 mm from the target surface, beyond which little or no emission is detected. Three dimensional plots of the variation of TOF signal with ambient pressure indicate that, close to the target surface, emission intensity is maximum for an ambient pressure of about 10 Torr. A double pulse experiment in which the second pulse reaches the plasma 4 ns after its creation reveals an increase in the velocities of the slower species, indicating coupling of optical energy to the plasma from the delayed laser pulse.

ACKNOWLEDGMENTS

Authors thank Jinto Thomas, Scientist, Institute for Plasma Research, Gandhinagar, for his valuable help and useful comments during the measurements.

[1]G. Ausanio, A. C. Barone, V. Iannotti, L. Lanotte, S. Amoruso, R. Bruzzese, and M. Vitiello, Appl. Phys. Lett. **85**, 4103 (2004).
[2]F. Claeyssens, S. J. Henley, and M. N. R. Ashfold, J. Appl. Phys. **94**, 2203 (2003).
[3]S. Amoruso, R. Bruzzese, X. Wang, N. N. Nedialkov, and P. A. Atanasov, J. Phys. D: Appl. Phys. **40**, 331 (2007).
[4]S. Amoruso, R. Bruzzese, N. Spinelli, R. Velotta, M. Vitiello, and X. Wang, Europhys. Lett. **67**, 404 (2004).
[5]S. Amoruso, G. Ausanio, R. Bruzzese, M. Vitiello, and X. Wang, Phy. Rev. B **71**, 033406 (2005).
[6]C. Thaury and F. Quéré, J. Phys. B: At. Mol. Opt. Phys. **43**, 213001 (2010).
[7]R. A. Ganeev, J. Phys. B: At. Mol. Opt. Phys. **40**, R213 (2007).
[8]C. Chenais-Popovics, O. Rancu, P. Renaudin, and J. C. Gauthier, Phys. Scr., T **65**, 163 (1996).
[9]S. S. Harilal, C. V. Bindhu, M. S. Tillack, F. Najmabadi, and A. C. Gaeris, J. Appl. Phys. **93**, 2380 (2003).
[10]B. Verhoff, S. S. Harilal, J. R. Freeman, P. K. Diwakar, and A. Hussanein, J. Appl. Phys. **112**, 093303 (2012).
[11]S. S. Harilal, A. Hassanien, D. Campos, P. Hough, and V. Sizyuk, J. Appl. Phys. **109**, 063306 (2011).
[12]S. S. Harilal, R. C. Issac, C. V. Bindhu, V. P. N. Nampoori, and C. P. G. Vallabhan, J. Appl. Phys. **80**, 3561 (1996).
[13]D. B. Geohegan, Appl. Phys. Lett. **60**, 2732 (1992).
[14]J. F. Keilkopf, Phys. Rev. E **52**, 2013 (1995).
[15]S. J. Henley, J. D. Carey, G. M. Fuge, M. N. R. Ashfold, and D. Anglos, Phys. Rev. B **72**, 205413 (2005).
[16]S. I. Anisimov, B. Kapeliovich, and T. Perel'man, JETP **39**, 375 (1994).
[17]S. Amoruso, R. Bruzzese, C. Pagano, and X. Wang, Appl. Phys. A **89**, 1017 (2007).
[18]T. A. Witten and L. M. Sander, Phys. Rev. Lett. **47**, 1400 (1981).
[19]See http://physics.nist.gov/PhysRefData/ASD/lines_form.html for NIST atomic spectra database.
[20]N. M. Shaikh, B. Rashid, S. Hafeez, Y. Jamil, and M. A. Baig, J. Phys. D: Appl. Phys. **39**, 1384 (2006).
[21]A. Couairon and A. Mysyrowicz, Phys. Rep. **441**, 47 (2007).
[22]S. S. Harilal, C. V. Bindhu, R. C. Issac, V. P. N. Nampoori, and C. P. G. Vallabhan, J. Appl. Phys. **82**, 2140 (1997).
[23]H. R. Griem, *Principles of Plasma Spectroscopy* (Cambridge University Press, Cambridge, 1997).
[24]M. S. Dimitrijevic and S. Sahal-Bréchot, Astron. Astrophys. Suppl. Ser. **140**, 193 (1999).
[25]R. W. P. McWhirter, *Plasma Diagnostic Techniques*, edited by R. H. Huddlestone and S. L. Leonard (Academic Press, New York, 1965), Chap. 5.
[26]H. Varel, M. Wähmer, A. Rosenfeld, D. Ashkenasi, and E. E. B. Campbell, Appl. Surf. Sci. **127–129**, 128 (1998).
[27]D. A. Cremers and L. J. Radziemski, *Handbook of Laser Induced Breakdown Spectroscopy* (John Wiley & Sons Ltd., 2006).